

Document downloaded from:

<http://hdl.handle.net/10251/83667>

This paper must be cited as:

Llopis Albert, C.; Merigó -Lindahl, JM.; Xu, Y. (2016). A coupled stochastic inverse / sharp interface seawater intrusion approach for coastal aquifers under groundwater parameter uncertainty. *Journal of Hydrology*. 540:774-783. doi:10.1016/j.jhydrol.2016.06.065.



The final publication is available at

<http://dx.doi.org/10.1016/j.jhydrol.2016.06.065>

Copyright Elsevier

Additional Information

# **A coupled stochastic inverse / sharp interface seawater intrusion approach for coastal aquifers under groundwater parameter uncertainty**

Carlos Llopis-Albert <sup>a</sup>; José M. Merigó<sup>b</sup>; Yejun Xu<sup>c</sup>

<sup>a</sup> Universitat Politècnica de València, C/ Camí de Vera s/n, 46022 Valencia, Spain; email: cllopisa@gmail.com

<sup>b</sup> Department of Management Control and Information Systems, University of Chile, Av. Diagonal Paraguay 257, 8330015 Santiago Chile, email: jmerigo@fen.uchile.cl

<sup>c</sup> Research Institute of Management Science, Business School, Hohai University, Nanjing 211100, PR China, email: xuyejohn@163.com

## **Abstract**

This paper presents an alternative approach to deal with seawater intrusion problems, that overcomes some of the limitations of previous works, by coupling the well-known SWI2 package for MODFLOW with a stochastic inverse model named GC method. On the one hand, the SWI2 allows a vertically integrated variable-density groundwater flow and seawater intrusion in coastal multi-aquifer systems, and a reduction in number of required model cells and the elimination of the need to solve the advective-dispersive transport equation, which leads to substantial model run-time savings. On the other hand, the GC method allows dealing with groundwater parameter uncertainty by constraining stochastic simulations to flow and mass transport data (i.e., hydraulic conductivity, freshwater heads, saltwater concentrations and travel times) and also to secondary information obtained from expert judgment or geophysical surveys, thus reducing uncertainty and increasing reliability in meeting the environmental standards. The methodology has been successfully applied to a transient movement of the freshwater-seawater interface in response to changing freshwater inflow in a two-aquifer coastal aquifer system, where an uncertainty assessment has been carried out by means of Monte Carlo simulation techniques. The approach also allows partially overcoming the

neglected diffusion and dispersion processes after the conditioning process since the uncertainty is reduced and results are closer to available data.

**Keywords:** Stochastic inversion; Gradual deformation; Seawater intrusion; Uncertainty; Reliability; Freshwater-seawater interface

## 1. Introduction

Seawater intrusion (SWI) is a major environmental threat and management challenge, especially in coastal aquifers supporting large populations, irrigated agriculture and industrial areas. SWI is probably the main cause of the high chloride content in areas located near the coast. For instance, the European Commission (80/778/EEC) has established a drinking water guideline value of 25 mg Cl/l. The excessive groundwater demand together with possible lower water availability because of climate change may lead to salinization of aquifers through the encroachment of seawater, which leads to a transition zone where the freshwater and saltwater mix and form an interface (e.g., Vandenbohede et al., 2010). This interface moves back and forth through time naturally because of fluctuations in the recharge and pumping rates. Furthermore, the concentration of the fluid within the transition zone is unknown, which makes the problem even more complex (Bear, 1999). The SWI problem can have major environmental impacts on water quality in both surface water and groundwater and also in their dependent ecosystems, particularly in over-exploited aquifers (e.g., Werner et al., 2012).

SWI problems is usually tackled in two ways. First is to use common simplifications, such as the sharp-interface approach and the Ghyben–Herzberg relation (Ghyben, 1889; Herzberg, 1901), because of its simplicity in terms of required parameters and computational burden. Although several authors have used this approach to deal with SWI problems in coastal aquifers the sharp interface approach disregard the diffusion and dispersion and should not be used where these processes are significant (Henry, 1964; Bear, 1979), and also the Ghyben–Herzberg relation can only be applied when the interface is practically stabilized, which means steady state flow conditions (Essaid, 1999). Several authors have used such approaches to deal with SWI problems in coastal aquifers (e.g., Strack, 1976; Dagan and Zeitoun, 1998; Cheng and Ouazar, 1999; Mantoglou et al., 2004; Pool and Carrera, 2011; Shi et al., 2011; Mas-Pla et al., 2013). Llopis-Albert and Pulido-Velazquez (2013) discussed the validity of sharp-interface models to deal

with SWI in coastal aquifers). In addition, some authors have used areal 2-D model by averaging the 3-D flow and transport equations vertically (Mass and Emke, 1998; Sorek et al., 2001; Pool et al., 2011) and boundary layer approximations (Paster and Dagan, 2007).

Second is to use variable-density models, but the scarcity of reliable estimates of parameters and variables (e.g., dispersion coefficients and saltwater concentrations) and the computational burden in most real cases prevents their use (Sreekanth and Datta, 2010). Furthermore, the computational burden implies a major disadvantage in coupled stochastic inverse-seawater models or coupled management simulation-optimization models for control and remediation of SWI due to multiple calls of the simulation model by the inverse or optimization algorithm (Dhar and Datta, 2009; Llopis-Albert, et al., 2014). However, in recent years, several works have substituted simulation models by approximate surrogate models (such as neural networks or genetic algorithms), efficient sampling strategies (e.g., optimized Latin hypercube sampling) or parallelization and grid computing to reduce the computational burden for solving groundwater management of SWI problems (e.g. Kourakos and Mantoglou, 2009; Ataie-Ashtiani et al., 2009; Lecca and Cao, 2009; Sreekanth and Datta, 2010; Sreekanth and Datta, 2011; Sreekanth and Datta, 2014; Rajabi and Ataie-Ashtiani 2014; Rajabi et al., 2015; Rajabi et al., 2015a; Ketabchi and Ataie-Ashtiani, 2015; Ketabchi and Ataie-Ashtiani, 2015a; Zhao et al., 2015). Ketabchi and Ataie-Ashtiani (2015b) and Singh (2015) carried out a review of SWI optimization-simulation problems.

Additionally, there are other works in the literature that have tackled the heterogeneity on seawater intrusion and performed comparisons of deterministic with stochastic approaches (Al-Bitar and Ababou, 2005; Held et al, 2005; Abarca, 2006; Carrera et al., 2009; Kerrou and Renard, 2010; Pool et al., 2015), which are in line with the present methodology.

Inverse calibration of coupled flow and transport models started a few decades ago and several reviews are available (Yeh 1986; Carrera 1987; McLaughlin and Townley 1996; Poeter and Hill 1997; de Marsily et al. 1999; Carrera et al. 2005; Zhou et al. 2014). However, there is still a limited literature regarding inverse calibration of SWI models (e.g., Iribar et al. 1997; Lebbe, 1999; Shoemaker 2004; Van Meir and Lebbe, 2005; Sanz and Voss, 2006; Carrera et al., 2010; Beaujean et al. 2014). Iribar et al. (1997) developed an automatic estimation of flow and transport parameters by means of a code that simulates flow and mass transport of constant density fluids. Lebbe (1999) developed a parameter identification in fresh-saltwater flow based on borehole resistivities and freshwater head data with the aim to identify horizontal and vertical

hydraulic conductivities, longitudinal and transversal dispersivities, and effective porosity in a homogeneous case. Shoemaker (2004) carried out a sensitivity analysis of density-dependent groundwater flow to provide insight about salt water intrusion calibration problems. Results showed that dispersivity is a very important parameter for reproducing a steady-state distribution of hydraulic head, salinity, and flow in the transition zone between fresh water and salt water in a coastal aquifer system. Van Meira and Lebbe (2005) presented an inverse tool for the simultaneous interpretation of the movement of the transition zone between saltwater and freshwater towards the pumping well and the evolution of the drawdowns at different depths and different distances from the pumping well. Sanz and Voss (2006) performed inverse modeling studies employing data collected from the classic Henry seawater intrusion for providing effective measurement strategies for estimation of parameters for seawater intrusion. Carrera et al. (2010) studied the computational and conceptual issues in the calibration of seawater intrusion models. It was found that despite the conceptual and computational difficulties, they can be partly overcome by using tidal response and electrical conductivity data. Ataie-Ashtiani et al. (2013) used the SUTRA (Voss and Provost, 2008) and the parameter estimation PEST (Doherty, 2005) models to deal with a real case saltwater intrusion problem. Beaujean et al. (2014) presented an inverse parameter estimation using surface electrical resistivity tomography and borehole data to evaluate the feasibility of identifying hydraulic conductivity and dispersivity in density dependent flow and transport models from surface Electrical resistivity tomography (ERT)-derived mass fraction. Llopis-Albert and Pulido-Velazquez (2015) used a sharp-interface approach and the PEST code to tackle SWI problems, with the advantage that by making use of a change of variable allows solving the equation with the classical MODFLOW code. Pool et al. (2015a) compared deterministic (i.e., geology-based zonation) and stochastic (using the regularized pilot points method of Alcolea et al., 2006) approaches for transmissivity inversion in a real regional coastal aquifer. This work goes a step further in the inverse modeling of the SWI problems since previous works use constant density fluids, are only applicable to homogeneous parameter estimation, present higher computational cost because of solving the advective-dispersive transport equation, only performed a sensitivity analysis to provide insight about salt water intrusion calibration problems, or not allow as much variety of data integration for uncertainty reduction.

Then this paper presents an alternative approach to deal with SWI problems by coupling the well-known Seawater Intrusion package (SWI2) (Bakker et al., 2013) for MODFLOW (McDonald and Harbaugh, 1988; Harbaugh et al. 2000) with an extension of the stochastic inverse model named GC method (Llopis-Albert,

2008; Capilla-Llopis Albert, 2009). The SWI2 allows a vertically integrated variable-density groundwater flow and seawater intrusion in coastal multi-aquifer systems. It allows a reduction in number of required model cells and the elimination of the need to solve the advective-dispersive transport equation, which leads to substantial model run-time savings.

The GC method deals with groundwater parameter uncertainty by constraining stochastic simulations to flow and mass transport data (i.e., hydraulic conductivity, freshwater heads and saltwater concentrations) and also to secondary information obtained from expert judgment or geophysical surveys, thus reducing uncertainty and increasing reliability in meeting the environmental standards. Furthermore, the GC method allows reproducing non-multi-Gaussian distributions and the existing preferential flow pathways, which is one of the most important issues in the management of coastal aquifers and the design of protection and correction actions (Carrera et al., 2010).

Although the SWI2 model disregards diffusion and dispersion processes the framework allows to partially overcoming this drawback. The methodology has been successfully applied to a transient movement of the freshwater-seawater interface in response to changing freshwater inflow in a two-aquifer coastal aquifer system, where an uncertainty assessment has been carried out by means of Monte Carlo simulation techniques.

The rest of the paper is organized as follows. Section 2 presents the description of the GC method and the SWI2 model. In section 3 the developed methodology is applied to a case study, while section 4 is devoted to the discussion of the results.

## **2. Modeling framework**

The methodology is based on the coupling of an extension of the stochastic inverse model named GC method with the SWI2 model, thus allowing to assess and reduce the uncertainty in heterogeneous aquifers and efficiently deal with three-dimensional vertically integrated variable-density groundwater flow and seawater intrusion in coastal multi-aquifer systems. An explanation of both models and the calibration procedure is provided below.

### **2.1. Gradual Conditioning (GC) method**

The Gradual Conditioning (GC) method constitutes a stochastic inverse modelling technique for the simulation of conductivity (K) fields, which has been widely applied to different environmental problems

in recent years. The theory of the GC method was initially presented by Llopis-Albert (2008) and Capilla and Llopis-Albert (2009). It was exhaustively verified on a 2D synthetic aquifer in Llopis-Albert and Capilla (2009), in which the simulation of  $K$  fields are conditional to  $K$  measurements, secondary information obtained from expert judgement and geophysical surveys, transient piezometric, solute concentration measurements, and travel time data. It was also applied to the Macrodispersion Experiment (MADE-2) site, which is a highly heterogeneous aquifer at Columbus Air Force Base in Mississippi (USA) (Llopis-Albert and Capilla, 2009a). This work showed the worth of the GC method to reproduce heavy tailing plume behaviors, the reduction of uncertainty results when conditioning to all available information, and the necessity of using a dual-domain mass transfer approach – or other transport equation different to the advection–dispersion equation (ADE) – when treating with upscaled models regardless of what random function is used to generate the  $K$  distribution. Additionally, the GC method allows tackling with complex real-world case studies of fractured rocks (Llopis-Albert and Capilla, 2010a), in which the capability of reproducing non-multi-Gaussian distributions and the existing preferential flow pathways. This is performed by means of the spatial correlation of extremely large/small  $K$  values that often take place in nature and can be crucial in order to obtain realistic and safe estimations of mass transport predictions. Furthermore, it was extended to deal with independent stochastic structures belonging to independent  $K$  statistical populations (SP) of fracture families and the rock matrix, each one with its own statistical properties (Llopis-Albert and Capilla, 2010b). Subsequently, the GC method was coupled with a management model for dealing with non-point agriculture pollution under groundwater parameter uncertainty (Llopis-Albert et al., 2014). It determines the spatial and temporal distribution of fertilizer application rates that maximizes net benefits in agriculture constrained by quality requirements in groundwater - for instance, those given by water laws such as the EU Water Framework Directive (WFD) - at various control sites, thus allowing obtaining the best management practices, the trade-off between higher economic returns and reliability in meeting the environmental standards, and more reliable policies on groundwater pollution control from agriculture. The structure adaptation of the  $K$  fields, while integrating the conditional information, was also analyzed in Llopis-Albert et al. (2015).

For the sake of conciseness, the reader is referred to those papers for all details of the methodology, and only a brief description of the GC methodology is here presented. The GC method uses a modified version of the gradual deformation technique (Hu, 2000; Hu et al., 2001; Hu, 2002), which consists of an iterative optimization process for constraining stochastic simulations to flow and mass transport data. This is carried

out by means of successive non-linear combinations of seed conditional realizations with the conditional K field resulting from the previous iteration. The procedure requires combining at least three conditional realizations at each iteration to ensure the preservation of mean, variance, variogram and data conditioning in the linearly combined field, for which linear combination coefficients must fulfil several constraints. The seed conductivity (K) fields are already conditional to K and secondary data and are generated by sequential indicator simulation. The a priori stochastic structure of these K seed fields is defined by means of the local cumulative density functions (ccdf's) and the indicator variograms, thus allowing the GC method to adopt any Random Function (RF) model. As a first step, the GC method builds linear sequential combinations of multiGaussian K fields that honour K data:

$$K^m = \alpha_1 K^{m-1} + \alpha_2 K_{2m} + \alpha_3 K_{2m+1} \text{ with } K^0 = K_1 \quad (1)$$

where subscripts stand for seed fields and superscripts for conditional fields resulting from a previous linear combination. That is, at m iteration, the field  $K^{m-1}$ , from the previous iteration, is combined with two new independent realizations  $K_{2m}$  and  $K_{2m+1}$ . The coefficients must fulfill the following constraints:

$$\begin{cases} \alpha_1 + \alpha_2 + \alpha_3 = 1 \\ (\alpha_1)^2 + (\alpha_2)^2 + (\alpha_3)^2 = 1 \end{cases} \quad (2)$$

being the parameterization of  $\alpha_i$  given by Eq. (3):

$$\begin{cases} \alpha_1 = \frac{1}{3} + \frac{2}{3} \cos \theta \\ \alpha_2 = \frac{1}{3} + \frac{2}{3} \sin(-\frac{\pi}{6} + \theta) \\ \alpha_3 = \frac{1}{3} + \frac{2}{3} \sin(-\frac{\pi}{6} - \theta) \end{cases} \text{ with } \theta \in [-\pi, \pi] \quad (3)$$

The  $\alpha_i$  coefficients are different in every iteration m, and correspond to a unique parameter  $\theta$ ; note the one to one correspondence between the parameter and the combined realization  $K^m$ . The avoidance of complex parameterizations is one of the most notorious features of the GC method, which leads to a high computational efficiency. Moreover, the mass transport equation is solved using a Lagrangian approach, thus avoiding the numerical dispersion usually found in Eulerian approaches, and includes a dual-domain mass transfer approach. The method also allows conditioning to travel time data through a backward-in-time probabilistic model (Neupauer and Wilson, 1999), which extends the applications of the method to the characterization of sources of groundwater contamination.



An extended version of the GC method has been developed to deal with variable density problems of seawater intrusion problems in coastal aquifers by coupling this inverse model with the SWI2 package (Bakker et al., 2013) for MODFLOW (McDonald and Harbough, 1988; Harbaugh et al. 2000), as further explained in the next section. The SWI2 output results used for the GC method at each iteration for conditioning stochastic simulations to data are the freshwater heads and the surface elevations for all cells of the spatial discretization (i.e., surfaces elevations representing interfaces or density isosurfaces, which separate zones with different density). Once the elevations are determined for each cell (note that in SWI2 package every aquifer can be represented by a single layer of cells, thus reducing the computational cost), the GC method interpolates those values to obtain the surfaces representing interfaces and the concentration at a specific coordinates of the domain can be calculated and compared with data. This approach can be followed for both the stratified and continuous options of the SWI2 package (see next sections for more details). As explained in Bakker et al. (2013), in the stratified option the water has a constant density in each zone, the density is discontinuous from zone to zone, and each surface represents an interface. Multiple interfaces may be used to separate, for instance, freshwater from brackish water, and brackish water from saltwater. In the continuous option, water density varies linearly in the vertical direction in each zone, density is continuous from zone to zone, the surfaces bounding the zones are density isosurfaces, and water density does not vary in the freshwater and saltwater zones. For both options initial values must be specified for all dependent variables in each aquifer (model layer) and include the freshwater head at the saturated top of each aquifer and the elevations of surfaces in each aquifer. Therefore, once the surfaces elevations are obtained the concentration values at a particular coordinate are easily computed (i.e., constant concentration between surface elevations in the stratified option and by piece-wise linear interpolation for the continuous one) and the penalty function at each iteration can be minimized. This function is made up by the weighted sum of three terms and penalizes the difference between computed and measured conditioning:

$$p^m(\theta) = p_h^m(\theta) + \Phi^m p_c^m(\theta) + \Psi^m p_\tau^m(\theta) \quad (4)$$

where  $p_h^m(\theta)$ ,  $p_c^m(\theta)$  and  $p_\tau^m(\theta)$  are the weighted sum of square differences between observed and calculated values for piezometric heads, concentrations and travel times, respectively. These terms are function of the parameter  $\theta$  (obtained at each iteration), for every time step  $t$  and measurement location  $i$ .

The terms  $\Phi^m$  and  $\Psi^m$  are trade-offs coefficients between the different conditioning data (see Capilla and Llopis-Albert, 2009).

Because the linear combination of independent non-Gaussian random functions does not preserve the non-Gaussian distribution, although the variogram is preserved, a transformation between Gaussian to the non-Gaussian fields (and vice versa) is required. This transformation is performed through the probability fields. The simulation procedure stops when a defined maximum number of optimization iterations is reached or a convergence criterion is achieved. It always converges to a global minimum due to the mutual independence of the seed fields when a sufficient number of iterations is used.

## **2.2. Brief description of the SWI2 package**

The Seawater Intrusion package (SWI2) has been exhaustively documented in Bakker et al. (2013), and consequently only a brief description of its capabilities is provided. It allows a three-dimensional vertically integrated variable-density groundwater flow and seawater intrusion in coastal multi-aquifer systems. This approach is based on the Dupuit approximation in which an aquifer is vertically discretized into zones of differing densities, separated from each other by defined surfaces representing interfaces or density isosurfaces. The numerical approach disregards the diffusion and dispersion and should not be used where these processes are significant. The resulting differential equations are equivalent in form to the groundwater flow equation for uniform-density flow, and hence, the MODFLOW code (McDonald and Harbaugh, 1988; Harbaugh et al., 2000) can be used. The approach only needs to add pseudo-source terms to deal with density effects, and has no need to solve the advective-dispersive transport equation. This is translated into the requirement of a single additional input file and modification of boundary heads to freshwater heads referenced to the top of the aquifer. By means of a combination of fluxes, after solving the groundwater flow equation and a simple tip and toe tracking algorithm, the vertical and horizontal movement of defined density surfaces is calculated separately. The SWI2 package allows dealing with fluid density within model layers using zones of constant density (stratified flow) or continuously varying density (piecewise linear in the vertical direction). Its main advantage in comparison to the variable-density groundwater flow and dispersive solute transport codes – such as SEAWAT (Guo and Langevin, 2002), FEFLOW (Diersch, 2002) or SUTRA (Voss and Provost, 2008) – is that fewer model cells are required, since every aquifer can be represented by a single layer of cells. Both the reduction in number of required

model cells and the elimination of the need to solve the advective-dispersive transport equation results in substantial model run-time savings, which can be large for regional aquifers. Furthermore, the computational cost of variable-density groundwater flow and dispersive solute transport codes would be unfeasible when embedded in a stochastic inverse model since they should be run hundreds of times. A comparison between SWI package and existing exact solutions and numerical solutions with SEAWAT was also performed by Dausman et al. (2010) and Bakker et al. (2013). The comparison led to successful results, and it was determined that when the diffusion and dispersion effects are important the use of the SWI package is discouraged.

### **3. Application to a case study**

We have used a synthetic case based on that presented in Bakker et al. (2013), thus allowing other researchers to compare their results using other inverse models since the input files for the deterministic case are provided in the SWI2 manual. In addition, the fact of using a synthetic case allows to have all variables under controlled conditions so that we can draw right conclusions from the analysis, and not being disturbed, e.g., by parameter uncertainty, lack of data, etc. The case study represents a transient movement of the freshwater-seawater interface in response to changing freshwater inflow in a two-aquifer coastal aquifer system. The example domain is 4,000 m long, 41 m high, and 1 m wide. The top and bottom of each aquifer is horizontal, being the top of the upper aquifer and bottom of the lower aquifer impermeable. The two aquifers are confined aquifers with 20 m thick each one and are separated by a leaky layer 1 m thick.

The spatial discretization consist of 200 columns that are each 20 m long, 1 row that is 1 m wide, and 3 layers that are 20, 1, and 20 m thick. The temporal discretization simulates 2,000 years using two 1,000-year stress periods, and a constant time step of 2 years. The stress periods are considered as steady-state, and thus storage changes are not simulated. With regard to the boundary conditions, the left 600 m of the model domain extends offshore, in which the ocean boundary is represented as a general head boundary (GHB) condition at the top of model layer 1. A freshwater head of 0 m is specified at the ocean bottom in all general head boundaries. The conductance that controls outflow from the aquifer into the ocean is 0.4 m<sup>2</sup>/d and corresponds to a leakance of 0.02 d<sup>-1</sup> (or a resistance of 50 days). The groundwater is divided into two zones, freshwater and seawater, separated by a surface interface that approximates the 50-percent seawater salinity contour. Fluid density is represented using the stratified density option, where the

dimensionless densities of the freshwater and saltwater are 0.0 and 0.025. The tip and toe tracking parameters are 0.04 and 0.02 respectively, while the *alfa* and *beta* parameters, as defined in the SWI2 package, are 0.1. The initial interface between freshwater and seawater is considered as straight, which is defined at the top of aquifer 1 at  $x = -100$ , and with a slope of  $-0.025$  m/m. The *isource* parameter is set to -2 in cells having GHBs so that water that infiltrates into the aquifer from the GHB cells is saltwater, whereas water that flows out of the model at the GHB cells is of the same type as the water at the top of the aquifer. In all other cells, this parameter is set to 0, indicating boundary conditions have water that is identical to water at the top of the aquifer.

An initial net freshwater inflow rate of  $0.03$  m<sup>3</sup>/d is specified at the right boundary, which causes flow to occur towards the ocean. For each layer the flow is distributed in proportion to the aquifer transmissivities. A freshwater source of  $0.01$  m<sup>3</sup>/d is specified in the right-most cell of the top aquifer for the first 1,000-year stress period, while a freshwater source of  $0.02$  m<sup>3</sup>/d is specified in the right-most cell of the bottom aquifer. These values are halved to reduce the net freshwater inflow to  $0.015$  m<sup>3</sup>/d during the second 1,000-year stress period. This flow is distributed in proportion to the transmissivities of both aquifers at the right boundary.

In order to address groundwater parameter uncertainty we have focused on the hydraulic conductivity ( $K$ ), since this is usually the parameter with the most significant spatial variation. In fact, it can vary spatially by several orders of magnitude. For instance, the aquifer at the Columbus Air Force Base in Mississippi, commonly known as the Macrodispersion Experiment (MADE) site, is a strongly heterogeneous system with a variance of the natural logarithm of  $K$  of nearly 4.5 (e.g., Llopis-Albert and Capilla, 2009a; Llopis-Albert et al., 2015a).

A stochastic Monte-Carlo approach is used to analyze the influence of heterogeneity in the seawater intrusion of coastal aquifers. For this, an ensemble of a hundred seed  $K$  fields is generated by means of sequential Gaussian simulation by means of the code GCOSIM3D (Gómez-Hernández and Journel, 1993). It is worthwhile mentioning that although the GC method allows defining any Random Function (RF) for the stochastic structure, a Gaussian distribution has been selected. This is because the domain has only one cell by layer and one row so that preferential flow paths are expected to have a low impact in the results. Therefore, the transformation between Gaussian to the non-Gaussian fields (and vice versa) is not required. In addition, the stochastic structure is assumed to be common for all simulated  $K$  fields, which simplifies the analysis avoiding the uncertainty on the stochastic structure. All  $K$  fields are equally likely realizations,

and hence, are plausible representations of reality, since they are conditional to the same  $K$  data and display the same degree of spatial variability. On the one hand, the stochastic structure has been defined by using a spherical variogram with a range approximately equal to  $1/20$  of the aquifer size for each direction. On the other hand, the Gaussian distribution is defined with a hydraulic conductivity mean ( $m$ ) for the top, confining unit and bottom aquifer of 2, 1 and 4 m/d, respectively; and a variance of  $m/2$  for each layer. The vertical hydraulic conductivity of the confining unit is 0.01 m/d, and the effective porosity is 0.2 for all model layers. One of these seed  $K$  fields has been chosen to be the true  $K$  field (i.e., it represents the actual heterogeneity in the aquifers). For the true  $K$  field, twenty hydraulic conductivity data ( $K$ ), freshwater heads ( $h_f$ ) and concentration values ( $c$ ) were obtained and used as conditioning data in the inverse model. These data were homogeneously distributed both spatially and temporally over the whole domain.

#### 4. Discussion and results

Fig. 1 shows for the true  $K$  field the initial and simulated freshwater-seawater interface for different times during the two stress periods. At the end of the first stress period (i.e., 1,000 years), the interface approaches its steady-state position. Fig. 1 also depicts the landward movement of the interface (to the right) caused by the reduction in freshwater flow towards the coast. At the end of the second period (2,000 years) the interface has not achieved a steady-state position in response to the reduction in freshwater flow toward the coast.

Note that the groundwater is divided into a freshwater zone and a seawater zone, separated by the sharp-interface surface between the zones that approximates the 50-percent seawater salinity contour (i.e. we use the “stratified” option of the SWI2 model) so that the concentration values for each cell can be inferred from the sharp-interface surface. Then model concentration ( $c$ ) fits regarding the true  $K$  field are compared for both seed and conditional  $K$  fields in different figures of the paper by means of the sharp-interface surfaces. Furthermore, it should be take into account that each aquifer is represented by a single layer of cells.

Fig. 2 presents the freshwater-seawater interface elevations for a hundred seed  $K$  field, the ensemble mean of those seed fields and the true  $K$  field. Because all seed  $K$  fields are equally likely realizations (i.e., they are plausible representations of reality since they are conditional to the same  $K$  data and display the same degree of spatial variability) the true  $K$  field falls within the bounds of the ensemble seed  $K$  fields. The

results show that the different interfaces present a certain uncertainty, leading to a wide range of values. In fact, the confining unit strongly affects the position of the interface in the upper and lower aquifers. In addition, the position of the interface is also affected by the effect of vertical resistance to flow, which can be related to different confining unit thicknesses and (or) different confining unit hydraulic properties. Furthermore, the greater the horizontal to vertical hydraulic conductivity ratio the higher is the difference regarding interface positions between SWI2 and variable-density groundwater flow and dispersive solute transport codes (Bakker et al., 2013). In this way, the maximum difference regarding the toe locations of fresh-seawater sharp interfaces for the seed  $K$  fields is around 300 meters. This uncertainty in the toe penetration of the freshwater-seawater interface of 300 meters can truly make a difference in meeting the environmental standards and regulations as established by lawmakers (Grima et al., 2015). Of course, this would also depend on the depth and rates of pumping wells. The problem could be worse in more complex aquifers with preferential flow paths, which would lead to further penetration of the interface inland.

Fig. 3 shows box-and-whisker plots depicting freshwater-seawater interfaces elevations for the seed  $K$  fields at different times and spatial locations in the X direction. The box-and-whisker plots show these elevations through their quartiles. That is, the 25<sup>th</sup> percentile, the median (i.e., the 50<sup>th</sup> percentile), the 75<sup>th</sup> percentile, and the remaining values up to and including the 5<sup>th</sup> and 95<sup>th</sup> percentiles. The boundaries of the boxes indicate the 25<sup>th</sup> percentiles and the 75<sup>th</sup> percentiles. The length of the box indicates the variability in the elevations. Then the larger the box, the greater the spread of model simulations and the more uncertainty in the model results (i.e., the freshwater-seawater interface elevations) as a consequence of the uncertainty in the hydraulic conductivity. The horizontal lines inside the boxes represent the medians. If a median is not in the center of the box, the distribution is skewed.

Results show there is higher uncertainty at early times and lower distances along the X direction. This is because the uncertainty is reduced when steady-state condition is being reached. In addition, results show that although the distribution of input parameters is Gaussian the distribution of output results (i.e., elevations) is skewed for many times and spatial locations (see Fig. 3). Elevations lying between the 5<sup>th</sup> and 95<sup>th</sup> percentiles are denoted by lines or whiskers extending from the bottom and top of each box, respectively. If the upper whisker is longer than the lower, it implies a positive skewness and vice versa. Elevations outside 5<sup>th</sup> and 95<sup>th</sup> percentiles are plotted as black circles, while the elevation of the true  $K$  field is represented as red circles. The true  $K$  field belongs to different percentiles through the time and spatial position, which reflects the high heterogeneity of the hydraulic conductivity used in this example.

Fig. 4 shows the freshwater-seawater interface elevations for a hundred conditional  $K$  field, the ensemble mean of those fields and the true  $K$  field. Results clearly show how the conditional simulations are closer to the true  $K$  field for all times, thus reducing uncertainty and increasing reliability in the freshwater-seawater interfaces.

Fig. 5 presents box-and-whisker plots depicting freshwater-seawater interfaces elevations for the conditional  $K$  fields at different times and spatial locations in the  $X$  direction. Again it is clear the reduction in uncertainty, since the length of the box-and-whiskers are shorter. Furthermore, although the true  $K$  field is not always within the 25<sup>th</sup> and 75<sup>th</sup> percentile in the seed  $K$  fields, after the conditional process this problem is corrected, thus showing the worth of the developed framework.

Additionally, the model fits to head ( $h$ ) and conductivity data ( $K$ ) for both seed and conditional simulations are provided for the whole domain. The criterion to evaluate simulation results is based on the performance measures of equation (5), which compare piezometric heads or concentrations obtained from solving the flow and transport equations with measurements (i.e., values from the true  $K$  field):

$$\eta_v = \sqrt{\frac{1}{m_v} \sum_{i \in m_v} \omega_{i,v} (v_i - v_i^m)^2} \quad (5)$$

The performance measure  $\eta_v$  corresponding to a variable  $v$ , representing either piezometric head ( $v = h$ ) or concentration ( $v = c$ ), computed at a given iteration  $k$  (having combined a total of  $2k+1$  seed fields), is defined as the square root of a weighted mean of the square departures of computed head or concentration ( $h$  or  $c$ ) from the measured heads ( $h^m$  or  $c^m$ ) after iteration  $k$ ; where  $m_v$  are the number of piezometric or concentration measurements and  $\omega_{i,v}$  the weights assigned to the piezometric or concentration measurements  $i$  ( $i=1, \dots, m_v$ ), which are defined to add up  $m_v$ . In the present work, we have used the same weight ( $\omega_{i,v}$ ) for all measurements; have calculated the performance measure  $\eta_v$  for all cells of the discretization; and only have presented  $\eta_h$  since the concentration for each cell can be inferred from the sharp-interface surfaces as presented in Fig. 1, 2, 4 and 7.

Eventually, the  $\eta_h$  at time  $t=1000$  years and for the ensemble seed  $K$  fields is 0.0049 and 0.0010 for the ensemble conditional  $K$  fields. Then a lower uncertainty is obtained after the conditioning process. Similar results are obtained for the other times of the simulation.

On the one hand, the ensemble seed  $K$  fields were generated with a mean ( $m$ ) for the top, confining unit and bottom aquifer of 2, 1 and 4 m/d, respectively; and a variance of  $m/2$  for each layer. On the other hand, the ensemble conditional  $K$  fields display a lower variance of approximately  $m/4$ .

These results have been achieved by using only a few conditioning data and after 25 iterations of the inverse model. Few data were selected to reproduce the scarcity of data in real SWI problems. Even better results would be expected if more conditional data or number of iterations would have been used. However, in real applications we should deal with: (1) the scarcity of available direct measurements of the hydrogeological parameters, (2) the need to integrate datasets of different types and scales and, (3) the inherent uncertainty associated to real groundwater systems.

The results are in line with those obtained by other researches, which stated that SWI is very sensitive to heterogeneity in hydraulic conductivity (e.g., Carrera et al., 2009). It is worthwhile mentioning that apart from the hydraulic conductivity, SWI also depends on the presence of preferential flow paths and aquifer bathymetry (Abarca et al. 2007), and is very sensitive to the dispersivity (Shoemaker, 2004). Narayan et al. (2007) also showed that seawater intrusion is far more sensitive to pumping rates and recharge than to aquifer properties such as hydraulic conductivity.

To better show the reduction of uncertainty after the conditioning process and the good agreement regarding the true  $K$  field, Fig. 6 depicts Fig. 4 (d) (i.e., freshwater-seawater interface elevations for a hundred conditional  $K$  field and their ensemble mean at  $t=2000$  years).

Additionally, Fig. 7 presents a comparison regarding the salt interface for the true  $K$  field at  $t=1000$  years between an analytical solution, using the Ghyben-Herzberg relation, and a numerical solution obtained using the developed stochastic approach. Furthermore, the comparison has been carried out when heterogeneity in  $K$  fields is considered, i.e., under groundwater parameter uncertainty. This figure shows the true  $K$  field, the ensemble mean (of 100  $K$  fields) for the simulated conditional  $K$  fields, and the ensemble mean (of 100  $K$  fields) for the analytical solutions (similar to the comparison performed by Al-Bitar and Ababou, 2005). On the one hand, results shows again the good agreement with regard to the salt interface of the true  $K$  field for the numerical solution using the developed stochastic approach. On the other hand, the analytical solution overestimates the toe penetration of the saltwater front. This is because it neglects the mixing zone and implicitly assumes that salt water remains static (e.g. Pool and Carrera, 2011; Llopis-Albert and Pulido-Velazquez, 2014). Eventually, similar results are obtained for other times.



## 5. Conclusions

Saltwater intrusion as a result of groundwater over-exploitation is a major concern in many coastal aquifers worldwide, which may lead to do not meet the environmental standards and regulations as established by lawmakers. This problem is further complicated by the existing uncertainty in groundwater parameters and the scarcity of available data. In order to provide reliable policies and to properly face the future climate change challenges there is a need for tools capable of integrating all available information and dealing with uncertainty. Note that expected water scarcity and higher water demand, because of the socio-economic development in coastal regions, will lead to an ever-increasing problem in the future as a consequence of the climate change. Then policy-makers can come up with the best management practices in terms of seawater penetration, transition zone width and critical pumping rates by using this tool.

Therefore this work goes a step further in the current literature by coupling the well-known SWI2 package for MODFLOW with a stochastic inverse model named GC method. The framework combines the advantages of both models. It allows to vertically integrate variable-density groundwater flow and seawater intrusion in coastal multi-aquifer systems with a reduced number of model cells and without the need to solve the advective-dispersive transport equation, which leads to substantial model run-time savings. In this way, the seawater intrusion model has been embedded into the inverse model to deal with groundwater parameter uncertainty by constraining stochastic simulations to flow and mass transport data (i.e., hydraulic conductivity, freshwater heads and saltwater concentrations) and also to secondary information obtained from expert judgment or geophysical surveys, thus reducing uncertainty and increasing reliability in meeting the environmental standards. The methodology has been successfully applied to a transient movement of the freshwater-seawater interface in response to changing freshwater inflow in a two-aquifer coastal aquifer system. An uncertainty assessment has been carried out by means of Monte Carlo simulation techniques, which has clearly shown a reduction of uncertainty and a good fit of the interfaces of the conditional simulations to that of the true  $K$  field. Furthermore, the framework allows partially overcoming the neglected diffusion and dispersion processes after the conditioning process, since the interfaces can be displaced to reproduce concentration data resulting of those processes.

## References

- Abarca, E. (2006). Seawater intrusion in complex geological environments, PhD thesis, Technical University of Catalonia, Spain.
- Abarca, E., Carrera, J., Sanchez-Vila, X., Dentz, M. (2007). Anisotropic dispersive Henry problem. *Advances in Water Resources* 30(4), 913–926.
- Al-Bitar, A., Ababou, R. (2005). Random field approach to seawater intrusion in heterogeneous coastal aquifers: unconditional simulations and statistical analysis. In: *Geostatistics for Environmental Applications*. Renard P., Demougeot-Renard H., Froidevaux R. (eds.), Springer Verlag.
- Alcolea, A., Carrera, J., Medina, A. (2006). Pilot points method incorporating prior information for solving the groundwater flow inverse problem. *Advances in Water Resources* 29, 1678–1689. Doi:10.1016/j.advwatres.2005.12.009.
- Ataie-Ashtiani, B., Ketabchi, H., Rajabi, M. (2014). Optimal management of freshwater lens in a small island using surrogate models and evolutionary algorithms. *ASCE Journal of Hydrological Engineering*, 19(2), 339-354.
- Ataie-Ashtiani, B., Rajabi, M., Ketabchi, H. (2013). Inverse modeling for freshwater lens in small islands: Kish island, Persian Gulf", *Hydrological Processes*, 27(19), 2759-2773.
- Bakker, M., Schaars, F., Hughes, J.D., Langevin, C.D., and Dausman, A.M., 2013. Documentation of the seawater intrusion (SWI2) package for MODFLOW: U.S. Geological Survey Techniques and Methods, book 6, chap. A46, 47 p., <http://pubs.usgs.gov/tm/6a46/>.
- Bakker, M., Essink, G.H.P., Langevin, C.D., 2004. The rotating movement of three immiscible fluids—A benchmark problem. *Journal of Hydrology*, 287, 271–279.
- Bear J. 1999. Conceptual and mathematical modeling. In *Seawater intrusion in coastal aquifers: concepts, methods, and practices*, Bear J, Cheng AH-D, Sorek S, Ouazar D, Herrera I. (eds). Kluwer Acad: Norwell, Mass; 127–161.
- Beaujean, J., Nguyen, F., Kemna, A., Antonsson, A., Engesgaard, P. (2014). Calibration of seawater intrusion models: Inverse parameter estimation using surface electrical resistivity tomography and borehole data. *Water Resources Research*, doi: 10.1002/2013WR014020.

- Carrera J. (1987). State of the art of the inverse problem applied to the flow and solute transport equations. In: Custodio E, Gurgui A, Ferreira JL, editors. Analytical and numerical groundwater flow and quality modelling. Series C, mathematical and physical sciences, vol. 224. Norwell, MA: D. Reidel.
- Capilla, J. E., Llopis-Albert, C. (2009). Gradual Conditioning of Non-Gaussian Transmissivity Fields to Flow and Mass Transport Data. *Journal of Hydrology*, 371, 66-74.
- Carrera J, Alcolea A, Medina A, Hidalgo J, Slooten L (2005). Inverse problem in hydrogeology. *Hydrogeology Journal*, 13, 206–222.
- Carrera, J., Hidalgo, J.J, Slooten, L.J., Vázquez-Suñé, E., (2009). Computational and conceptual issues in the calibration of seawater intrusion models. *Hydrogeology Journal*, 18, 131–145. Doi: 10.1007/s10040-009-0524-1.
- Cheng AH-D, Ouazar D. (1999). Analytical solutions. In *Seawater intrusion in coastal aquifers: concepts, methods, and practices*, Bear J, Cheng AH-D, Sorek S, Ouazar D, Herrera I. (eds). Kluwer Acad: Norwell, Mass; 163–191.
- Dagan G, Zeitoun DG. (1998). Seawater–freshwater interface in a stratified aquifer of random permeability distribution. *Journal of Contaminant Hydrology* 29(3): 185–203. DOI: 10.1016/S0169-7722 (97)00013-2.
- de Marsily, G., Delhomme, J.P., Delay, F., Buoro, A. (1999). 40 years of inverse problems in hydrogeology. *CR Acad Sci Paris Earth Planet Sci* 329(2), 73–87.
- Diersch H-JG. (2002). FEFLOW finite element subsurface flow and transport simulation system reference manual. Report No. WASY Institute for Water Resources Planning and Systems Research.
- Doherty J. 2005. PEST: model independent parameter estimation, user manual. 5th edn. Watermark Numerical Computing.
- Essaid HI. 1999. USGS SHARP model. In *Seawater intrusion in coastal aquifers – concepts, methods and practices*, Bear J, Cheng AH-D, Sorek S, Ouazar D, Herrera I. (eds). Kluwer Acad: Norwell, Mass.
- Ghyben, W.B., 1889, Nota in verband met de voorgenomen putboring nabij Amsterdam: *Tijdschrift van het Koninklijk Instituut van Ingenieurs*, p. 8–22.
- Gómez-Hernández, J.J., Journel, A.G., 1993. Joint simulation of multi-Gaussian random variables. In: Soares, A. (Ed.), *Geostatistics Tróia '92*, vol. 1. Kluwer, pp. 85e94.

- Gómez-Hernández, J.J., Wen, X.H., 1998. To be or not to be multiGaussian? A reflection on stochastic hydrogeology. *Adv. Water Resour.* 21 (1), 47–61.
- Grima, J., Luque-Espinar, J.A., Mejía, J.A., Rodríguez, R. (2015). Methodological approach for the analysis of groundwater quality in the framework of the Groundwater Directive. *Environmental Earth Sciences*, 74(5). DOI: 10.1007/s12665-015-4472-x.
- Guo W, Langevin CD, 2002. User's guide to SEAWAT: a computer program for simulation of three-dimensional variable-density groundwater flow. Report No. US Geol. Surv. Open File, 01-434.
- Harbaugh, A.W., Banta, E.R., Hill, M.C. and McDonald, M.G. (2000). MODFLOW- 2000, The U.S. Geological Survey modular groundwater model-User guide to modularization concepts and the groundwater flow process. US Geol. Surv. Open-File Rep 00–92, 12.
- Held, R., Attinger, S., Kinzelbach, W. (2005). Homogenization and effective parameters for the Henry problem in heterogeneous formations. *Water Resources Research*, 41, W11420, doi:10.1029/2004WR003674.
- Henry HR. 1964. Effects of dispersion on salt encroachment in coastal aquifers, U.S. Geol. Surv. Water Supply Pap., 1613-C.
- Herzberg, A., 1901, Die Wasserversorgung einiger Nordseebäder: *Journal für Gasbeleuchtung und Wasserversorgung*, v. 44, p. 815–819.
- Herckenrath, D., Langevin, C.D., Doherty, J. (2011). Predictive uncertainty analysis of a saltwater intrusion model using null-space Monte Carlo, *Water Resour. Res.*, 47, W05504, doi:10.1029/2010WR009342.
- Hu, L.Y. (2000). Gradual deformation and iterative calibration of Gaussian related stochastic models. *Mathematical Geology*, 32 (1), 87–108.
- Hu, L.Y, Blanc, G. and Noetinger, B. (2001). Gradual deformation and iterative calibration of sequential stochastic simulations. *Mathematical Geology*, 33, 475-490.
- Hu, LY (2002). Combination of dependent realizations within the gradual deformation method. *Mathematical Geology*, 34(8), 953–963.
- Iribar, V., Carrera, J., Custodio, E., Medina, A., (1997). Inverse modelling of seawater intrusion in the Llobregat delta deep aquifer. *Journal of Hydrology* 198, 226–244.

- Kerrou, J., Renard, P., (2010). A numerical analysis of dimensionality and heterogeneity effects on advective dispersive seawater intrusion processes. *Hydrogeology Journal*, 18(1), 55-72.
- Ketabchi, H., Ataie-Ashtiani, B. (2015). Assessment of a parallel evolutionary optimization approach for efficient management of coastal aquifers. *Environmental Modeling and Software*, 74, 21-38.
- Ketabchi, H., Ataie-Ashtiani, B. (2015a). Evolutionary algorithms for the optimal management of coastal groundwater: A comparative study toward future challenges", *Journal of Hydrology*, 520, 193-213.
- Ketabchi, H., Ataie-Ashtiani, B. (2015b). Review: Coastal groundwater optimization—advances, challenges, and practical solutions. *Hydrogeology Journal* 23(6), 1129-1154.
- Kourakos G, Mantoglou A. (2009). Pumping optimization of coastal aquifers based on evolutionary algorithms and surrogate modular neural network models. *Advances in Water Resources* 32(2009): 507–521.
- Lecca, G., Cao, P., 2009. Using a Monte Carlo approach to evaluate seawater intrusion in the Oristano coastal aquifer: a case study from the AQUAGRID collaborative computing platform. *Phys. Chem. Earth, Parts A/B/C* 34 (10), 654–661. Doi: 10.1016/j.pce.2009.03.002.
- Llopis-Albert, C. (2008). Stochastic inverse modeling conditional to flow, mass transport and secondary information. Edited by Universitat Politècnica de València (Spain). ISBN: 978-84-691-9796-7.
- Llopis-Albert, C. and Capilla, J.E. (2009). Gradual Conditioning of Non-Gaussian Transmissivity Fields to Flow and Mass Transport Data. Demonstration on a Synthetic Aquifer. *Journal of Hydrology*, 371, 53-55.
- Llopis-Albert, C. and Capilla, J.E., (2009a). Gradual Conditioning of Non-Gaussian Transmissivity Fields to Flow and Mass Transport Data. Application to the Macrodispersion Experiment (MADE-2) site, on Columbus Air Force Base in Mississippi (USA). *Journal of Hydrology*, 371, 75-84.
- Llopis-Albert, C. and Capilla, J.E. (2010a). Stochastic simulation of non-Gaussian 3D conductivity fields in a fractured medium with multiple statistical populations: a case study. *Journal of Hydrologic Engineering*, 15(7), 554-566.

- Llopis-Albert, C. and Capilla, J.E. (2010b). Stochastic inverse modeling of hydraulic conductivity fields taking into account independent stochastic structures: A 3D case study. *Journal of Hydrology*, 391, 277–288.
- Llopis-Albert, C., Palacios-Marqués, D., Merigó, J.M. (2014). A coupled stochastic inverse-management framework for dealing with nonpoint agriculture pollution under groundwater parameter uncertainty. *Journal of Hydrology* 511, 10–16.
- Llopis-Albert, C., Pulido-Velazquez, D. (2014). Discussion about the validity of sharp-interface models to deal with seawater intrusion in coastal aquifers. *Hydrological Processes* 28(10), 3642–3654. doi: 10.1002/hyp.9908.
- Llopis-Albert, C., Pulido-Velazquez, D. (2015). Using MODFLOW code to approach transient hydraulic head with a sharp-interface solution. *Hydrological Processes*, 29(8), 2052–2064. doi: 10.1002/hyp.10354.
- Llopis-Albert, C., Merigó, J.M, Palacios-Marqués, D. (2015). Structure Adaptation in Stochastic Inverse Methods for Integrating Information. *Water Resources Management* 29(1), 95-107. doi: 10.1007/s11269-014-0829-2.
- Llopis-Albert, C., Palacios-Marqués, D., Soto-Acosta, P. (2015a). Decision-making and stakeholders' constructive participation in environmental projects. *Journal of Business Research* 68, 1641–1644. doi: 10.1016/j.jbusres.2015.02.010.
- Mantoglou A, Papantoniou M, Giannouloupoulos P. 2004. Management of coastal aquifers based on nonlinear optimization and evolutionary algorithms. *Journal of Hydrology* 297(1-4): 209–228. DOI: 10.1016/j.jhydrol.2004.04.011.
- Maas, C., Emke, M. (1988). Solving varying density groundwater problems with a single density computer program, *Natuurwet. Tijdschr*, 70, 143-154.
- Mas-Pla J, Rodríguez-Florit A, Zamorano M, Roqué C, Menció A, Brusi D. (2013). Anticipating the effects of groundwater withdrawal on seawater intrusion and soil settlement in urban coastal areas. *Hydrological Processes* 27(16): 2352–2366. DOI: 10.1002/hyp.9377
- McDonald, M. G., & Harbaugh, A. W. (1988). A modular three-dimensional finite-difference groundwater flow model. US Geological Survey Technical Manual of Water Resources Investigation, Book 6, US Geological Survey, Reston, Virginia, 586.

- McLaughlin D., Townley, L.L.R. (1996). A reassessment of the groundwater inverse problem. *Water Resources Research*, 32(5), 1131–1161.
- Narayan, K.A., Schleeberger, C., Bristow, K.L. (2007). Modelling seawater intrusion in the Burdekin Delta Irrigation Area, North Queensland, Australia. *Agricultural water management* 89, 217–228.
- Neupauer, R.M. and Wilson, J.L. (1999). Adjoint method for obtaining backward-in-time location and travel time probabilities of a conservative groundwater contaminant. *Water Resources Research* 35 (11), 3389–3398.
- Paster, A., Dagan, G. (2007). Mixing at the interface between two fluids in porous media: A boundary-layer solution. *Journal of Fluid Mechanics*, 584, 455-472.
- Peña-Haro, S., Llopis-Albert, C., Pulido-Velazquez, M. (2010) Fertilizer standards for controlling groundwater nitrate pollution from agriculture: El Salobral-Los Llanos case study, Spain. *Journal of Hydrology* 392(3): 174–187.
- Peña-Haro, S., Pulido-Velazquez, M., Llopis-Albert, C. (2011). Stochastic hydro-economic modeling for optimal management of agricultural groundwater nitrate pollution under hydraulic conductivity uncertainty. *Environmental Modelling & Software* 26 (8), 999-1008.
- Poeter, E.P., Hill, M.C. (1997). Inverse models: a necessary next step in groundwater modeling. *Ground Water* 35(2), 250–260.
- Pool M, Carrera J. (2011). A correction factor to account for mixing in Ghyben–Herzberg and critical pumping rate approximations of seawater intrusion in coastal aquifers. *Water Resources Research* 47: W05506. DOI: 10.1029/2010WR010256.
- Pool, M., Carrera, J., Dentz, M. Hidalgo, J.J., Abarca, E. (2011). Vertical average for modeling seawater intrusion. *Water Resources Research*, 47, W11506, doi:10.1029/2011WR010447.
- Pool, M., Post, V. E. A., Simmons, C.T. (2015). Effects of tidal fluctuations and spatial heterogeneity on mixing and spreading in spatially heterogeneous coastal aquifers. *Water Resources Research*, 51, 1570-1585.

- Pool, M., Carrera, J., Alcolea, A., Bocanegra, E.M. (2015a). A comparison of deterministic and stochastic approaches for regional scale inverse modeling on the Mar del Plata aquifer. *Journal of Hydrology*, 531, 214-229.
- Pulido-Velazquez, D.; Llopis-Albert, C.; Peña-Haro, S.; Pulido-Velazquez, M. (2011). Efficient conceptual model for simulating the effect of aquifer heterogeneity on natural groundwater discharge to rivers. *Advances in Water Resources*, doi:10.1016/j.advwatres.2011.07.010.
- Rajabi, M., Ataie-Ashtiani, B. (2014). Sampling efficiency in Monte Carlo based uncertainty propagation strategies: Application in seawater intrusion simulations. *Advances in Water Resources*, 67(6), 46-64.
- Rajabi, M., Ataie-Ashtiani, B., Simmons, C.T. (2015). Polynomial Chaos Expansions for Uncertainty Propagation and Moment Independent Sensitivity Analysis of Seawater Intrusion Simulations. *Journal of Hydrology*, 520, 101-122.
- Rajabi, M., Ataie-Ashtiani, B., Janssen, H. (2015a). Efficiency enhancement of optimized Latin hypercube sampling strategies: Application to Monte Carlo uncertainty analysis and meta-modeling. *Advances in Water Resources*, 76, 127-139.
- Sanz, E., Voss, C.I. (2006). Inverse modeling for seawater intrusion in coastal aquifers: Insights about parameter sensitivities, variances, correlations and estimation procedures derived from the Henry problem. *Advances in Water Resources* 29, 439–457.
- Shi L, Cui L, Park N, Huyakorn PS. (2011). Applicability of a sharpinterface model for estimating steady-state salinity at pumping wells – validation against sand tank experiments. *Journal of Contaminant Hydrology* 124(1-4): 35–42. DOI: 10.1016/j.jconhyd.2011.01.005.
- Shoemaker, G.B. (2004). Important Observations and Parameters for a Salt Water Intrusion Model. *Ground Water*, Vol. 42(6), 829–840.
- Sorek, S., Borisov, V.S., Yakirevich, A. (2001). A two-dimensional areal model for density dependent flow regime. *Transport in Porous Media*, 43(1), 87-105.
- Sreekanth J, Datta B. (2010). Multi-objective management of saltwater intrusion in coastal aquifers using genetic programming and modular neural network based surrogate models. *Journal of Hydrology*, 393, 245–256.



- Sreekanth, J., Datta, B. (2011). Coupled simulation-optimization model for coastal aquifer management using genetic programming-based ensemble surrogate models and multiple-realization optimization, *Water Resources Research*, 47, W04516, doi:10.1029/2010WR009683.
- Sreekanth J., Bithin Datta (2014): Stochastic and robust multi-objective management of pumping from coastal aquifers under parameter uncertainty. *Water Resources Management*, 28, 2005-2019. Doi: 10.1007/s11269-014-0591-5.
- Strack ODL. 1976. A single potential solution for regional interface problems in coastal aquifers. *Water Resources Research* 12:1165–117. DOI: 10.1029/WR012i006p01165
- Van Meira, N., Lebbe, L. (2005). Parameter identification for axi-symmetric density-dependent groundwater flow based on drawdown and concentration data. *Journal of Hydrology* 309, 167–177.
- Vandenbohede, A., L. Lebbe, R. Adams, E. Cosyns, P. Durinck, Zwaenepoel, A. (2010). Hydrological study for improved nature restoration in dune ecosystems-Kleyne Vlakte case study, Belgium. *Journal of Environmental Management*, 91(11), 2385–2395, doi:10.1016/j.jenvman.2010.06.023.
- Voss CI, Provost AM. (2008). SUTRA, a model for saturated-unsaturated variable density groundwater flow with energy or solute transport. U.S. Geological Survey, Water-Resources Investigations, Open-File Report. 87–4369.
- Yeh, W.W.G. (1986). Review of parameter estimation procedures in groundwater hydrology: the inverse problem. *Water Resources Research*, 22, 95–108.
- Werner, A. D., Bakker, M., Post, V. E. A. , Vandenbohede, A., Lu, C., Ataie-Ashtiani, B., Simmons, C. T., Barry, D.A. (2012). Seawater intrusion processes, investigation and management: Recent advances and future challenges. *Advances in Water Resources*, 51, 3–26, doi:10.1016/j.advwatres.2012.03.004.
- Zhao, Z., Zhao, J., Xin, P., Jin, G., Hua, G., Li, L. (2015). A Hybrid Sampling Method for the Fuzzy Stochastic Uncertainty Analysis of Seawater Intrusion Simulations. *Journal of Coastal Research*. Doi: 10.2112/JCOASTRES-D-15-00084.1.
- Zhou, H., Gómez-Hernández, J.J., Li, L. (2014). Inverse methods in hydrogeology: Evolution and recent trends. *Advances in Water Resources* 63, 22–37. Doi: 10.1016/j.advwatres.2013.10.014.

## FIGURE CAPTIONS

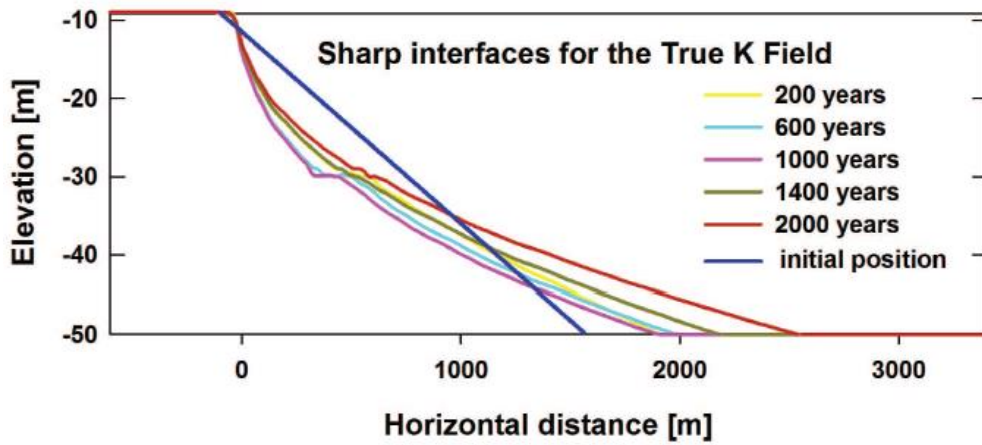


Fig 1. Simulated freshwater-seawater interface elevations for different times.

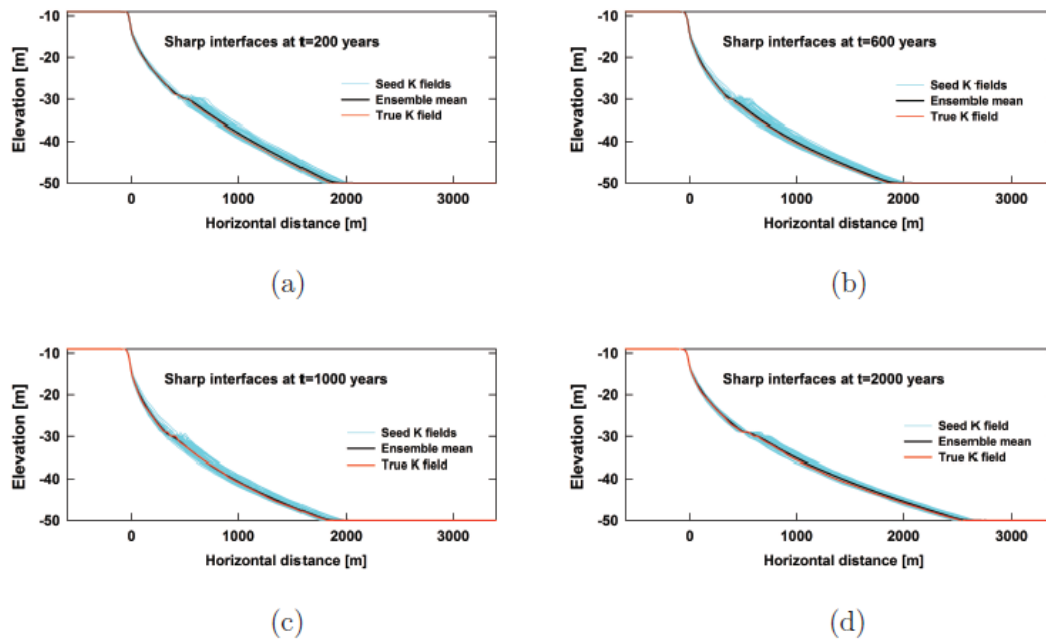


Fig 2. Simulated freshwater-seawater interface elevations for the seed  $K$  fields, their ensemble mean and the true  $K$  field at different times.

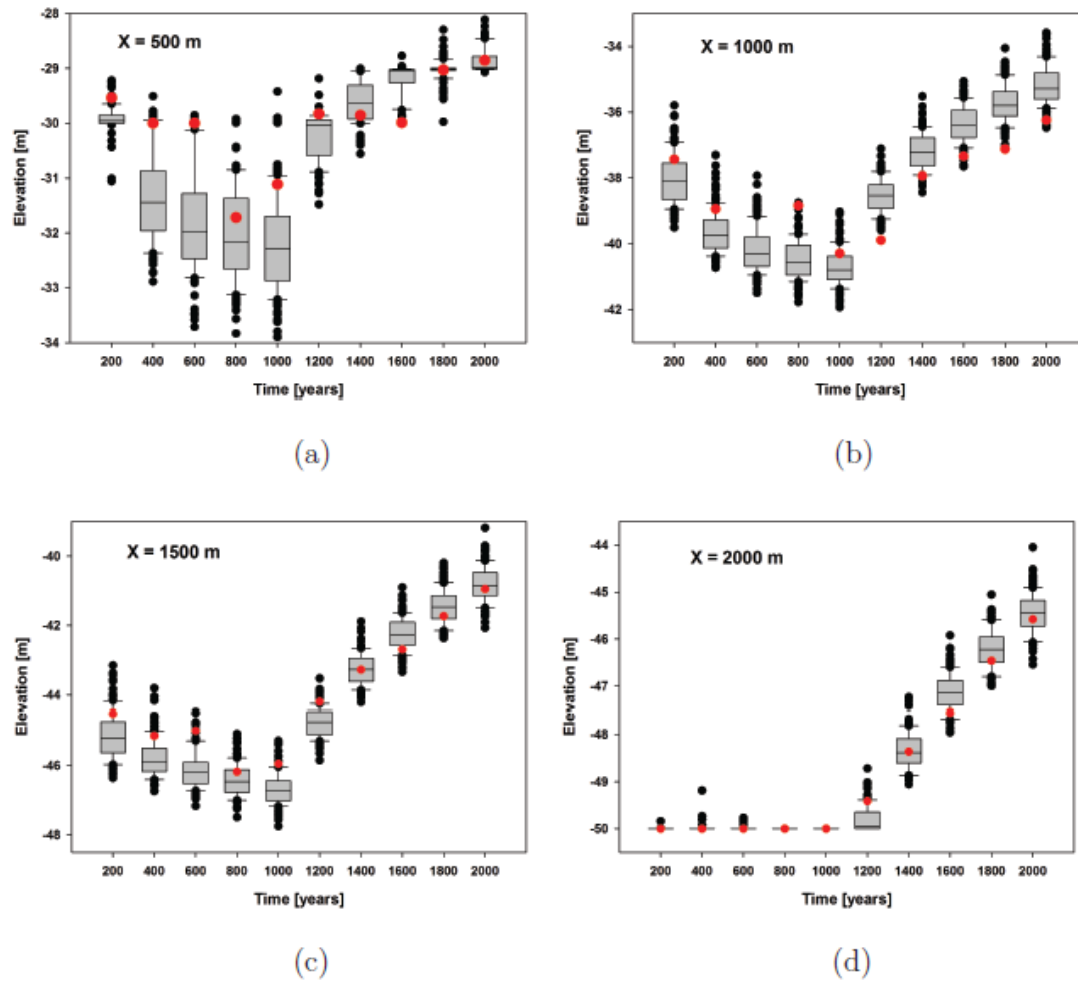


Fig. 3. Box-and-whisker plots depicting freshwater-seawater interfaces elevations for the seed  $K$  fields at different times and spatial locations. Elevations outside 5<sup>th</sup> and 95<sup>th</sup> percentiles are plotted as black circles, while the elevation of the true  $K$  field is represented as red circles.

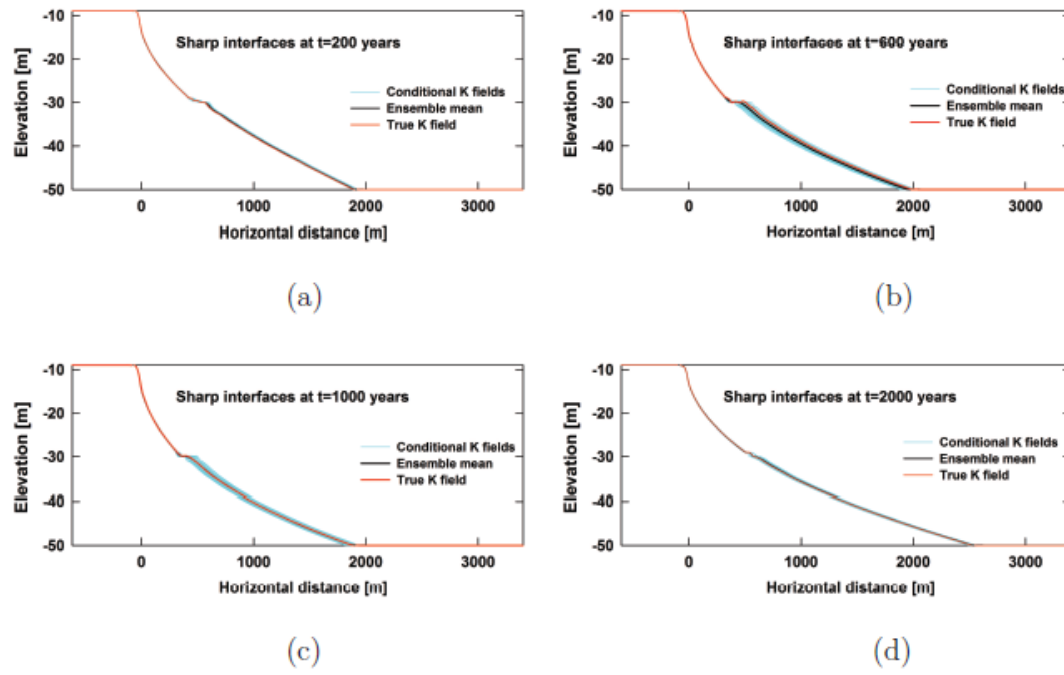


Fig 4. Simulated freshwater-seawater interface elevations for the conditional  $K$  fields, their ensemble mean and the true  $K$  field at different times.

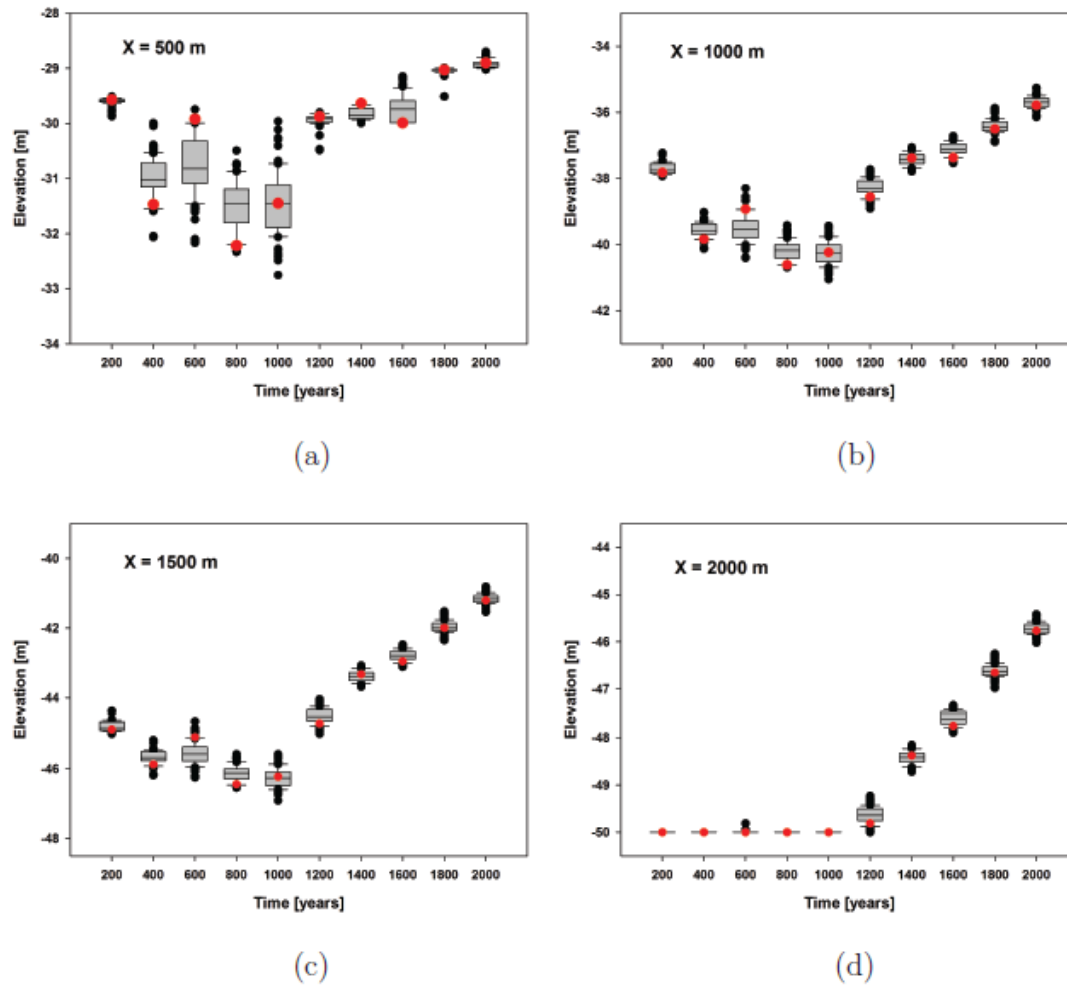


Fig. 5. Box-and-whisker plots depicting freshwater-seawater interfaces elevations for the seed  $K$  fields at different times and spatial locations. Elevations outside 5<sup>th</sup> and 95<sup>th</sup> percentiles are plotted as black circles, while the elevation of the true  $K$  field is represented as red circles.

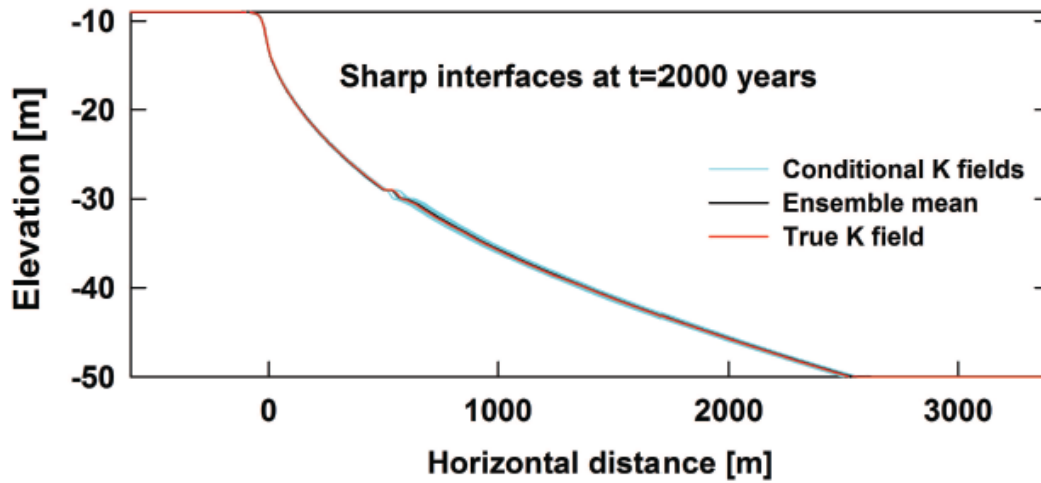


Fig. 6. Simulated freshwater-seawater interface elevations for the conditional  $K$  fields, their ensemble mean and the true  $K$  field at  $t=2000$  years.

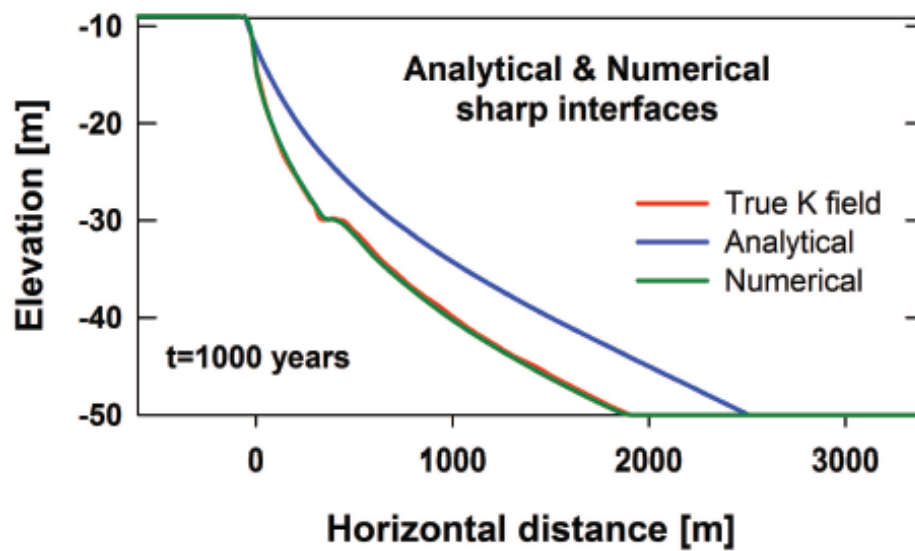


Fig. 7. Comparison regarding the salt interface between analytical and numerical solutions.